HNPS Advances in Nuclear Physics

Vol 2 (1991)

HNPS1991

NUCLEAR MOMENTUM DISTRIBUTION WITH FRACTIONAL OCCUPATION PROBABILITIES OF THE SURFACE ORBITS

T. S. Kosmas, J. D. Vergados

doi: 10.12681/hnps.2849

NUCLEAR MOMENTUM DISTRIBUTION WITH FRACTIONAL OCCUPATION PROBABILITIES OF THE SURFACE ORBITS

T. S. KOSMAS[1,2] and J. D. VERGADOS[1]

1 Division of Theoretical Physics, University of Ioannina, GR 451 10 Ioannina, Greece

2 Institute of Theoretical Physics II, University of Bochum, D 4630 Bochum, Germany

Abstract

Simplified expressions for calculating nucleon momentum distributions are derived in the context of the harmonic oscillator shell model and in its modification in which fractional occupation probabilities of the surface orbits are used. The method is applied to study the proton momentum distribution of the spherical nucleus ^{40}Ca. The values of the partial occupation probabilities used had been previously determined by fitting to the experimental elastic form factor data.

1. Introduction

During the last decade the nucleon momentum distribution $\eta(\mathbf{k})$, where $\mathbf{k}$ the momentum transfer, has received considerable attention mainly on the theoretical side [1-5]. The main reason for these studies is the sensitivity of momentum distribution to the correlations, a fact that makes it one of the best places to investigate the significance of the various sorts of correlations [6-8]: short-range and long-range, tensor-correlations etc. Theoretically, $\eta(\mathbf{k})$ is studied by using independent-particle models and other self consistent methods (for a recent review see ref. [7]). The single particle results in the nuclear ground state, can be corrected and improved by including two-nucleon correlations in the closed shell configuration of the ground state or by assuming fractional occupation probabilities for the valence orbitals [9-11] which to some extent take into account the effect of the different sorts of correlations.

In this work, we derive simple expressions for the nucleon momentum distribution $\eta(\mathbf{k})$ similar to those found in ref. [11,12] for the form factor and charge distribution in the context of the shell model. Then by exploiting these expressions we calculate $\eta(\mathbf{k})$

by assuming that the surface nucleons of a nucleus are distributed in the valence orbitals (j-levels) with fractional occupation probabilities described by ajustable parameters. The method is applied to the double closed shell nucleus ^{40}Ca and the effect of the use of partial occupation probabilities on $\eta(\mathbf{k})$ is estimated.

2. Independent-particle formalism

On the basis of the independent-particle shell model (IPSM) the proton (neutron) momentum distribution $\eta(\mathbf{k})$, assuming that the ground state of a nucleus (A.Z) is well described by a Slater determinant. is obtained by the following expression

$$\eta(\mathbf{k}) = \sum_{n,l,j} \mid \tilde{\Psi}_{nlj}(\mathbf{k}) \mid^2 \tag{1}$$

where $\tilde{\Psi}_{nlj}(\mathbf{k})$ is the Fourier transform of the single point-nucleon spatial wavefunction $\Psi_{nlj}(\mathbf{r})$ with quantum numbers n, l and j. For the most of the closed (sub)shell nuclei $\eta(\mathbf{k})$ is in a good approximation spherically symmetric. Then, the more interesting radial momentum distribution $\eta(k)$, is given by

$$\eta(k) = \frac{1}{4\pi} \sum_{(n,l)j \text{ occupied}} (2j+1) \mid \tilde{R}_{nlj}(k) \mid^2 \tag{2}$$

with

$$\tilde{R}_{nlj}(k) = i^l \left(\frac{2}{\pi}\right)^{\frac{1}{2}} \int_0^\infty j_l(kr) R_{nlj}(r)\, r^2 dr \tag{2a}$$

$j_l(x)$ is the Bessel function of order l and $R_{nlj}(r)$ is the radial part of the single particle wavefunction. For harmonic oscillator (h.o.) wave functions from eq. (2a) we get

$$\tilde{R}_{nlj}(k) = i^l (-)^n \sqrt{\frac{2n!\, b^3}{\Gamma(n+l+\frac{3}{2})}} (kb)^l\, e^{-\frac{(kb)^2}{2}}\, L_n^{l+\frac{1}{2}}(k^2b^2) \tag{3}$$

with $L_n^\beta(x)$ being a Laguerre polynomial and b the h.o. parameter. In this case after further elaboration of eq. (2) we can interchange the summations [11,12], so as it can be rewritten in the simple form

$$\eta(k) = \frac{b^3}{\pi^{3/2}}\, e^{-(kb)^2}\, \Pi(kb, Z) \tag{4}$$

where $\Pi(\chi, Z)$ is defined as

$$\Pi(\chi, Z) = \sum_{\lambda=0}^{N_{max}} f_\lambda \chi^{2\lambda}, \qquad \chi = kb \tag{4a}$$

Thus, $\Pi(\chi, Z)$ is a polynomial of even powers in the momentum transfer k. In eq. (4a) $N_{max} = (2n + l)_{max}$, is the maximum number of oscillator quanta occupied by protons (neutrons) and f_λ are coefficients defined as

$$f_\lambda = \sum_{(n,l)j,\ \lambda \geq l} \frac{\pi^{\frac{1}{2}}(2j+1)n! C_{nl}^{\lambda-l}}{2\Gamma(n+l+\frac{3}{2})} \tag{4b}$$

Z (N)	Upper j-level	$\lambda = 0$	$\lambda = 1$	$\lambda = 2$	$\lambda = 3$	$\lambda = 4$
2	$0s_{1/2}$	2				
6	$0p_{3/2}$	2	8/3			
8	$0p_{1/2}$	2	4			
14	$0d_{5/2}$	2	4	8/5		
16	$1s_{1/2}$	5	0	44/15		
20	$0d_{3/2}$	5	0	4		
28	$0f_{7/2}$	5	0	4	64/105	
32	$1p_{3/2}$	5	20/3	-4/3	176/105	
38	$0f_{5/2}$	5	20/3	-4/3	64/3	
40	$1p_{1/2}$	5	10	-4	8/3	
50	$0g_{9/2}$	5	10	-4	8/3	32/189

Table 1. A list of coefficients f_λ of eq. (4b), which give the proton (neutron) momentum distributions for closed (sub)shell nuclei with $Z \leq 50$ (or $N \leq 50$), by using expressions (4), (8), and (9) (see text).

with C_{nl}^{m} given by (see eq. (A.9) of ref. [13]).

$$C_{nl}^{m} = \sum_{\kappa=0}^{m} \frac{(-)^{m}}{\kappa!(m-\kappa)!} \binom{n+l+\frac{1}{2}}{n-\kappa} \binom{n+l+\frac{1}{2}}{n+\kappa-m} \tag{4c}$$

Obviously the determination of the polynomial $\Pi(\chi, Z)$ is sufficient in order to calculate the independent-particle momentum distribution $\eta(k)$. Though h.o. shell model calculations have been often employed previously [2,5,7], the general formulae (4)-(4b) have not been constructed. Only a few forms of eq. (4) have been written for light nuclei in ref. [7] p. 50.

Using eqs. (4)-(4b), the proton and neutron momentum distributions can be expressed simply for all closed (sub)shell nuclei. Values of the coefficients f_{λ} for nuclei up to Sn isotopes are listed in table 1 (see ref. [11] for others), from which we can see that they are simple rational numbers. A comparison of eq. (4b) with eq. (3a) of ref. [11] shows that the same coefficients f_{λ} can be also used for the calculation of the charge distribution in closed (sub)shell nuclei.

3. Study with fractional occupation probabilities

In section 2 we assumed that the occupation probabilities of the j-levels are unity for states below the Fermi level and zero above it. It is well known that even spherical nuclei like ^{40}Ca, do not have good closed shells and nuclear Fermi surface appears to be diffused. Here we shall construct general expressions for calculating the nucleon momentum distribution in the case when the filling numbers of the surface orbits are not integers but fractional numbers described by parameters. In this way we can study the effect of the partial occupation probabilities in the momentum distribution. The parameters can be determined by fitting to the experimental data for the charge form factor.

In the case when fractional occupation probabilities are assumed, the average momentum distribution is written as (see e.g. ref. [3]).

$$\eta(k) = \frac{1}{4\pi} \sum_{(n,l)j} (2j+1) a_{nlj} \mid \tilde{R}_{nlj}(k) \mid^{2} \tag{6}$$

where the sum runs over all the quantum numbers (n,l)j of the single particle states with proton (neutron) occupation probabilities a_{nlj}. For the "core orbits" below the Fermi level of the nucleus $a_{nlj} = 1$, namely, they are equal to the independent-particle predictions, but

for the "active (surface) orbits" $a_{nlj} < 1$. Also $a_{nlj} \neq 0$ for some orbits above the Fermi level, which according to the independent-particle picture they are empty. The following normalization relations hold

$$\sum_{(n,l)j \ closed} (2j+1) \ = \ \sum_{all \ (n,l)j} (2j+1)a_{nlj} \ = \ N_n \tag{7}$$

$N_n = Z$ (*or* N) for the proton (neutron) case. We use separate normalization relations for proton or neutron momentum distribution ($4\pi \int \eta(k)k^2dk = N_n$).

From eqs. (4) and (6) we can derive simple parametric expressions with one, two, three etc. parameters describing the deviation of filling numbers from those of the simple shell model ones. With the aid of these parametric expressions we can calculate $\eta(k)$ of a nucleus and investigate the effect of the nuclear surface diffuseness on this property.

For an approximately spherical nucleus (A,Z) (even when this is an open-shell nucleus), assuming that only two filling numbers of the states are non-integers, the corresponding one-parameter formula giving the nucleon momentum distribution, is written as

$$\Pi(\chi, Z, \alpha_1) = \Pi(\chi, Z_1) + \Big[\Pi(\chi, Z_c) - \Pi(\chi, Z_1)\Big] \frac{Z_c - Z_1 - \alpha_1}{Z_c - Z_1} +$$

$$\Big[\Pi(\chi, Z') - \Pi(\chi, Z_c)\Big] \frac{Z - Z_c + \alpha_1}{Z_c - Z_1} \tag{8}$$

The polynomials $\Pi(\chi, Z_i)$ determine the momentum distribution of three adjacent closed shell nuclei in the frame of IPSM. More precisely, $\Pi(\chi, Z)$ describes $\eta(k)$ of the considered nucleus; $\Pi(\chi, Z_c)$ describes $\eta(k)$ of the closed (sub)shell nucleus with $Z_c \leq Z$ having as upper occupied level the one lying just below the Fermi level of the nucleus (A,Z) and $\Pi(\chi, Z')$ describes $\eta(k)$ of the closed (sub)shell nucleus with $Z' > Z$ having as upper occupied level the one lying just above the Fermi level of the nucleus (A,Z). The last two terms in eq. (8) contain the contributions of the two active surface levels with occupation numbers $Z_c - Z_1 - \alpha_1$ and $Z - Z_c + \alpha_1$ respectively. Thus, the parameter α_1 determines the depletion of the level just below the Fermi surface of the considered nucleus and the increase of the occupation number for the first level above it [11].

Eq. (8) can be extended to a two-, three- etc. parametric equation describing $\eta(k)$ by means of the partial occupation probabilities of the j-orbitals. As an example we assume that the surface nucleons of a nucleus with $20 \leq Z \leq 28$ are spread on four partially

occupied subshells: $1s_{\frac{1}{2}}$, $0d_{\frac{3}{2}}$, $0f_{\frac{7}{2}}$ and $1p_{\frac{3}{2}}$. In the single particle shell model picture the first two of them are fully occupied and the other two are empty. Then the three-parametric polynomial we must put in the place of $\Pi(\chi, Z)$ in eq. (4), is given by

$$\Pi(\chi, Z, \alpha_1, \alpha_2, \alpha_3) = \frac{10 - 3\alpha_1}{2} + \frac{11\alpha_1 + 5\alpha_2 - 5\alpha_3}{3}\chi^2 +$$

$$\frac{60 - 10\alpha_1 - 29\alpha_2 + 25\alpha_3}{15}\chi^4 + \frac{8Z - 160 + 28\alpha_1 + 28\alpha_2 - 20\alpha_3}{105}\chi^6 \qquad (9)$$

Eq. (9) by putting Z=20 gives the three-parametric equation for proton (neutron) momentum distribution of ^{40}Ca. Furthermore by putting $\alpha_1 = 0$ and $\alpha_2 = \alpha_3$ we get the corresponding one-parameter expression for $\eta(k)$ in the case when fractional filling numbers for the subshells $0d_{\frac{3}{2}}$ and $0f_{\frac{7}{2}}$ surface orbitals are assumed.

4. Results and discussion

The method described above was applied to calculate the proton (neutron) momentum distribution of the core nucleus ^{40}Ca. We assumed that the surface protons for ^{40}Ca are distributed on the partially occupied subshells $1s_{\frac{1}{2}}$, $0d_{\frac{3}{2}}$, $0f_{\frac{7}{2}}$ and $1p_{\frac{3}{2}}$. We used eq. (9) with Z=20 and we took $b = 1.998\, fm^{-1}$ which reproduces the experimental value of the rms radius [11] of ^{40}Ca and the values for the parameters α_i: $\alpha_1 = .65$, $\alpha_2 = .45$, and $\alpha_3 = .75$ determined by fitting to the charge form factor in ref. [11]. The respective occupation numbers correspond to 5.5% depletion of the Fermi sea, which is much lower than the recent calculation of Mahaux and Sartor [8] who obtained occupation values 13% for the $0f_{\frac{7}{2}}$ orbital and 9% for the $1p_{\frac{3}{2}}$ orbital and 20-25% depletion of the s-d valence shells or 10-12.5% depletion of the Fermi sea.

The results for the proton momentum distribution $\eta(k)$ are shown in fig. 1 (dashed line) where for comparison the results obtained by putting $\alpha_i = 0$, i.e. the simple shell model results (full line) are also shown. We see that the fractional occupation probabilities for the surface orbits slightly change the h.o shell model results.

It is well known that the momentum distribution is strongly affected by explicit insertion of various sorts of correlations [1-5,13,14]. In ref. [2] it was found that short range correlations modify significantly the independent particle shell model momentum distribution for low momenta and dominate it for high momenta. In the works of refs. [3,8] a different method was developed and it was shown that by varying the occupation probabilities of single particle orbits one can investigate the effects associated with various types

of correlations. It was also shown how correlations introduced into the charge density distribution can be used for evaluating the momentum distribution.

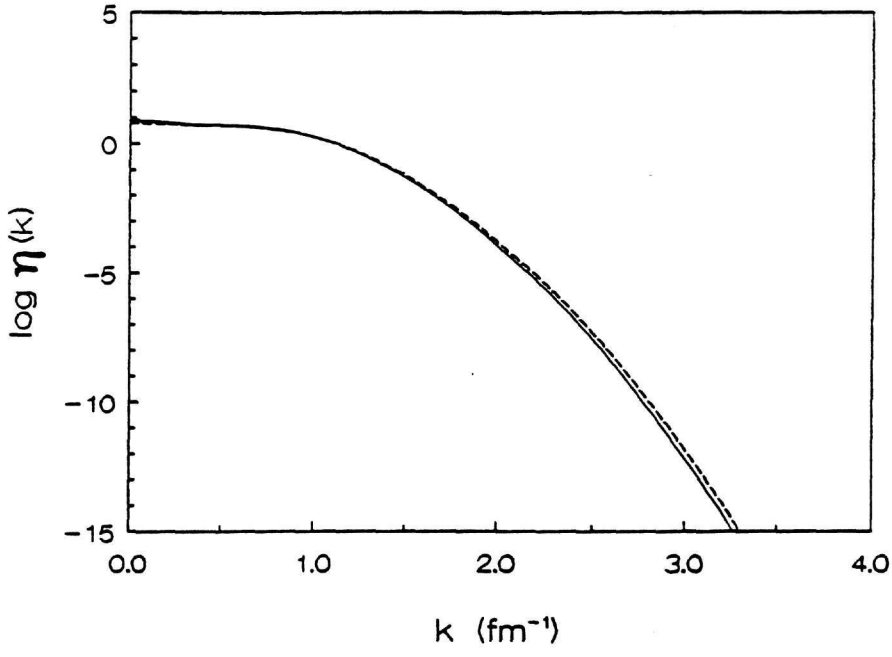

Fig. 1. Proton momentum distribution for ^{40}Ca calculated with the independent particle h.o. shell model (full line) and by assuming fractional occupation probabilities for four surface j-levels (dashed line).

Our results show that, even if fractional occupation probabilities are assumed, the density distributions calculated from the single-particle shell model do not include all effects of short range correlations and high momentum components which dominate the momentum distribution. These components are absent not only from the momentum distribution (fig. 1) but also from the form factor (fig. 2 of ref. [11]) and they have to be explicitly taken into account.

5. Summary and conclusions

In this work, by using h.o. wavefunctions we find simplified expressions for studying the proton and neutron momentum distribution $\eta(k)$ for all closed (sub)shell nuclei of the periodic table. By exploiting the independent-particle formalism we constructed modified

expressions by introducing fractional occupation probabilities of the surface orbits.

From tentative calculations for ^{40}Ca we estimated the influence of fractional occupation probabilities on $\eta(k)$ and we concluded the following: Although the used partial filling numbers of the surface levels change significantly the IPSM results of charge distribution and form factor and improve the reproducibility of the experimental data, they do not change essentially the IPSM results of momentum distribution. This is so because. inclusion of fractional occupation probabilities does not change the single particle wavefunctions. Nucleon momentum distribution is dominated by the short range correlations, which in the present work are only effectively taken into account.

References

[1] J. G. Zabolitzky and W. Ey, Phys. Lett. B 76 (1978) 527

[2] J. W. Van Orden, W. Truex and M. K. Banerjee, Phys. Rev. C 21(1980)2628

[3] C. J. Jaminon, C. Mahaux and H. Ngo, Phys. Lett. B 158 (1985) 103; Nucl. Phys. A 440 (1985) 228; Nucl. Phys. A 473 (1987) 585

[4] O. Benhar. C. Giofi Degli Atti, S. Liuti and G. Salme, Phys. Lett. B 177 (1986) 135

[5] A. N. Antonov, I. Zh. Petkov and P. E. Hodgson, Nuovo Cim. A, 97 (1987) 117
A. N. Antonov, E. N. Nikolov, Chr. V. Cristov, I. Zh. Petkov and P. E. Hodgson. Nuovo Cim. A 102 (1989) 1701

[6] V. R. Pandharipande, C. N. Papanicolas and J. Wambach, Phys. Rev. Lett. 53 (1984) 1133

[7] A. N. Antonov, P. E. Hodgson and I. Zh. Petkov, "Nucleon momentum distribution in nuclei", (Clarendon Press, Oxford, 1988).

[8] C. J. Jaminon, C. Mahaux and H. Ngo, Nucl. Phys. A 452 (1986) 445
C. Mahaux and R. Sartor, Nucl. Phys. A 484 (1988) 205

[9] F. Malaguti et al. Riv. Nuovo Cim. 5 (1982) 1

[10] I. S. Gulkarov, M. M. Mansurov and A. A. Khomich, Sov. J. Nucl. Phys. 47 (1988)25

[11] T. S. Kosmas and J. D. Vergados, Proc. 1st Hellenic Symposium in Theoretical Nuclear Physics, Thessaloniki, Greece, (University Press, 1990)

[12] T. S. Kosmas and J. D. Vergados, Phys. Lett. B 215 (1988) 460; Nucl. Phys. A 510 (1990) 641

[13] S. Boffi O. Nicrosini and M. Radici, Nucl. Phys. A 490 (1988) 585

[14] S. Stringari. M. Triani and O. Bohigas, Nucl. Phys. A. 516 (1990) 33

APPLICATION OF ACCELERATOR-BASED TECHNIQUES TO THE CHARACTERIZATION AND ANALYSIS OF NEAR-SURFACE LAYERS OF MATERIALS

Panagiotis MISAELIDES

Department of Chemistry, Aristotle University, GR-54006 Thessaloniki, Greece.

Abstract

Small accelerators are finding growing interest as analytical tool in the surface characterization of materials supporting industrial processes. A variety of accelerator-based nuclear analytical techniques have been developed during the last years allowing the determination of traces of light elements (ppm-und ppb-concentrations) and their depth distribution in the near-surface layers of materials. During this contribution the application of nuclear analytical techniques to the determination of the bulk concentration and depth distribution of oxygen will presented as an example of the variety of possible low energy nuclear reactions and interactions, that can be used for the study of surface phenomena.

1. Introduction

During the last two decades the basic nuclear physics research work performed using small accelerators has drastically decreased indicating the need of a new field of activity or the shut-down of these mashines. The low-energy beam accelerators spread in numerous universities and research laboratories found an interesting field of application as analytical tool supporting developments in non-nuclear disciplines. A variety of accelerator- based analytical techniques have been established allowing the test of the influence of the elemental constitution of near-surface layers of materials on their properties and characteristics. This is due to the inherent atomic and nuclear properties of the ion beams. The ions gradually slow down in the material in a well defined way so that their velocity or energy at any point gives a direct evidence of the material layer traversed. The rate of slow down depends on the ion species, its initial energy and the material matrix concerned. In this way keV- or MeV-energy ions from small accelerators can be used as an analytical probe for the "interfacial" region between the surface, that can be examined using optical spectroscopy and atomic or slow-ion techniques, and the bulk. There are numerous reviews in the literature discussing in details the theoretical and practical basis of these techniques [e.g. 1, 2, 3, 4, 5]. This type of work also contributes to the basic nuclear physics research by the evaluation, test and, eventually, precision measurement of nuclear data, especially differential cross-sections, widths of narrow

resonances and decay data.

During this contribution the application of nuclear analytical techniques to the determination of the bulk concentration and depth distribution of oxygen will presented as an example of the variety of accelerator-based methods, that can be used for the characterization and analysis of materials surfaces. These methods find especial application to the semiconductor industry and to the metallurgy. The experimental work connected with this contribution was performed using the Tandem Accelerator of the NCSR Democritos and the 2.5 and 7 MV van der Graaff accelerators of the Nuclear Physics Institute of the University of Frankfurt a.M./Germany.

2. The Techniques

The determination of trace amounts of light elements using the conventional techniques of chemistry and optical spectroscopy is very difficult. In the case of oxygen the IR-spectroscopy can be used in the semiconductor industry for the determination of ppm and sub-ppm amounts of oxygen after calibration of the system using an absolute determination technique like a nuclear method. The determination of the depth distribution of elements on materials surfaces using classical analytical techniques is impossible.

The techniques applied for the determination of oxygen in near-surface layers of materials can be distinguished in two major groups:

1. **Techniques suitable for the determination its bulk concentration and**
2. **Techniques allowing the determination its depth distribution**

Among the techniques of the first group the **Charged Particle Activation Analysis** (**CPAA**) and the **Photon Activation Analysis** (**PAA**) are most popular especially semiconductor industry for the absolute calibration of conventional analytical techniques (e.g. FT-IR spectroscopy). Both techniques are suitable for the determination of light elements and are characterized by high selectivity and sensitivity.

The basic concept of CPAA is similar with the much widely spread thermal neutron activation analysis (INAA). The only difference in the formula providing the concentration (g) of the element to be determined is the consideration of the energy loss of the projectiles in the matrix material and the corresponding correction of the cross-section.

$$g = \frac{A * M}{N_A * \Phi * (1 - e^{-\lambda t}) * H * \int_{E_T}^{E_I} \sigma(E) * (\rho * \frac{dS}{dE}) * dE}$$

where A : the intensity of radiation emitted by the sample after an activation of duration t
M : atomic mass of the element to be determined
H : abundance of the isotope concerned
N_A : Avogadro number
Φ : particle fluency (can be calculated from the collected ion beam current integral)
$\sigma(E)$: cross-section
ρ : density of the matrix
$\frac{dS}{dE}$: stopping power of the projectiles
λ : decay constant of reaction product ($\lambda = \ln 2 / T_{1/2}$)

Different nuclear reactions are suitable for the determination of traces of oxygen in semiconductor matrices [6,7,8]. The selection of the reaction and the projectile energy for every case depends on the matrix material and the possible interference from other elements present expected (s. Table 1)

Table 1: The most usual reactions used for the determination of trace amounts of oxygen in semiconductor matrices

REACTION	REACTION PRODUCT	$T_{1/2}$	RADIATION EMITTED
$^{16}O(d,n)$	^{17}F	1.08 min	β^+
$^{16}O(^3He,p)$	^{18}F	109.6 min	β^+
$^{16}O(^3He,n)$	$^{18}Ne \rightarrow ^{18}F$	109.6 min	β^+
$^{16}O(t,n)$	^{18}F	109.6 min	β^+

Especially interesting for the determination of oxygen in semiconductor matrices are the last three reactions leading to the β^+-emitter ^{18}F. The measurement of the annihilation radiation (511 keV) as a function of the time provides the means of the quantitative determination. The limits of detection achieved without any chemical and thermal treatment of the sample (except the controled removal of a contaminated by the accelerator gases thin surface layer of a few microns) are of the order of few ppb depending on the matrix material.

The ^3He- and deuteron activations simultaneously lead to the quantitative determination of boron, carbon, nitrogen and silicon by the corresponding nuclear reactions given in Table 2.

A requirement for the determination of oxygen and generally using the technique of CPAA is the homogeneity of the target material and good knowledge of the reaction cross sections. The last fact had as consequence the high-precision redetermination of the cross-sections of number of nuclear reactions studied in the fifties and sixties.

In the Fig. 1 the decay of the 511 keV radiation of a GaAs-sample irradiated by 3.5 MeV deuterons is given as a function of

The ^3He-activation of traces of oxygen in especially samples can be also used for calibration purposes. Fig. 2 gives the calibration curve of the absorption coefficient α of the IR spectroscopy as a function of the absolute oxygen content of the silicon samples determined by CPAA [10]

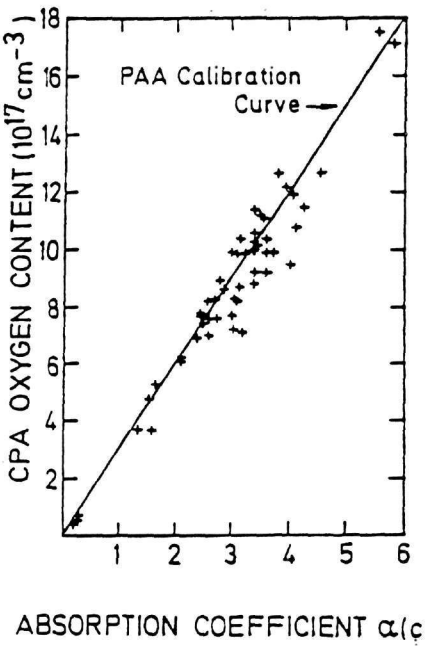

Fig. 2 : Correlation of the absorption coefficient of the of the IR-spectroscopy with the absolute concentration of oxygen in the sample determined by CPAA [10].

The prompt γ-radiation (937, 1040 and 1080 keV) emitted during the bombardment of ^{16}O with ^3He-ions (deexcitation of the first excited states of ^{18}F produced by the reaction: $^{16}O(^3He,p\gamma)^{18}F$) was also used for the determination of the depth distribution of oxygen on materials surfaces [9]. Depth distribution information can be also obtained by neutron spectroscopy during the bombardment of ^{16}O with deuterons using a time-of-flight technique [10]. The Q-values for the two groups of neutrons emitted are -1.624 MeV (for n_0) and -2.119 MeV (for n_1).

The Photon Activation Analysis uses the $^{16}O(\gamma,n)^{15}O$ nuclear reaction for the determination of oxygen [11]. The photons are produced by the bombardment of a tungsten target by 30 MeV electrons. The energy distribution of the Bremsstrahlung produced has a maximum in the energy area of 20 MeV exciting the ^{16}O-nucleus and inducing the neutron emission (giant resonance). The PAA has

been also used for the same calibration purposes as the CPAA in the semiconductor industry.

The determination of the depth distribution of the oxygen in near-surface layers of materials can be performed by a variety of techniques. Apart from the more exotic methods mentioned before the Nuclear Reaction Analysis (NRA), the Nuclear Resonant Reaction Analysis (NRRA), the Rutherford Backscattering Spectrometry (RBS), the Resonant Scattering Spectrometry (RSS) and the Elastic Recoil Detection Analysis (ERDA) are the most common techniques for the determination of the depth distribution of oxygen on material surfaces. The basic idea of all these techniques is almost the same. A particle with an initial energy E_{p0} reaches a depth x below the surface of a material with an energy E_p and induces then an interaction with a target atom (oxygen in this case). The interaction can be a nuclear reaction or a scatter process. The emitted particle or recoil nucleus with an energy E_{x0} at the depth x traverses the material and reaches a detector system with an energy E_x (s. Fig.3)

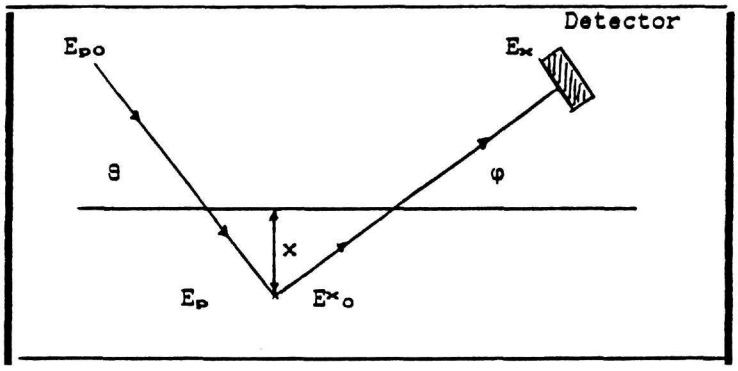

Fig. 3: Schematic representation of the techniques providing information about the depth distribution of oxygen on materials surfaces.

The energy E_p depends on the initial energy E_{p0}, the angle ϑ, the stopping power of the particle in the material matrix and the depth x. The energy of the emitted species at the depth x, E_{x0}, depends on the energy E_p, the nuclear properties of the target nucleus and projectile and the kind of interaction. The final energy E_x of the ejectiles reaching the detector system set at an angle φ depends on the energy E_{x0}, the angle φ and the energy loss of the ejectile traversing the material layer.

The Nuclear Reaction Technique is the most popular technique for the determination of light element profiles on materials surfaces. In the case of ^{16}O the (d,p_0)-, (d,p_1)- and (d,α)-reactions [e.g. 12, 13] available for this purpose. The positive Q-values of 1.919, 1.048 and 3.116 MeV respectively make these

the time. The decay curves with half-lives of 9.96, 2.03 and 1.08 min belong to the ^{13}N, ^{15}O and ^{17}F formed by the activation carbon, nitrogen and oxygen.

Table 2: Nuclear reactions enabling the simultaneous determination of traces of other light trace elements in semiconductor matrices.

REACTION	REACTION PRODUCT	$T_{1/2}$	RADIATION EMITTED
$^{10}B(d,n)$	^{11}C	20.3 min	β^+
$^{10}B(^3He,pn)$	^{11}C	20.3 min	β^+
$^{11}B(^3He,n)$	^{13}N	9.96 min	β^+
$^{12}C(d,n)$	^{13}N	9.96 min	β^+
$^{12}C(^3He,\alpha)$	^{11}C	20.3 min	β^+
$^{14}N(d,n)$	^{15}O	2.03 min	β^+
$^{14}N(^3He,\alpha)$	^{13}N	9.96 min	β^+
$^{28}Si(^3He,n)$	$^{30}S \rightarrow ^{30}P$	2.50 min	β^+
$^{28}Si(^3He,p)$	^{30}P	2.50 min	β^+

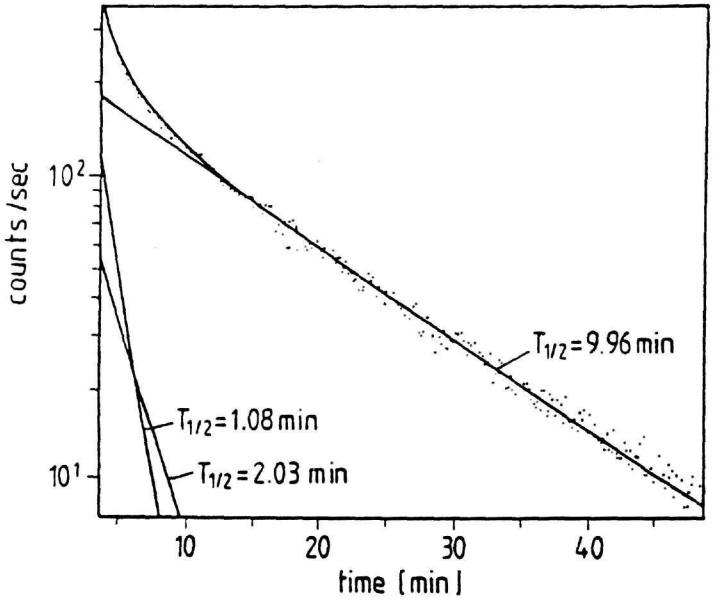

Fig. 1 : Decay of the annihilation radiation of a GaAs sample irradiated by 3.5 MeV deuterons.

reactions suitable also for low-energy beam accelerators. These reactions were frequently used in the past for the study of numerous surface phenomena (oxidations, corrosion) on a variety of material matrices and are still widely used for the solution of complicated material science problems on metal and semiconductor matrices. The Fig. 4 shows the proton-spectra and the corresponding oxygen profiles of oxidized Zr-samples treated for 1 and 2 days at 650 °C in comparison with the untreated oxidized sample. [14]. Studies of this type can lead to the determination of diffusion coefficients and corrosion properties of materials in different environments. The Radiochemical Laboratory is studying at the moment the oxidation of implanted and non-implanted stainless-steels in aggresive environments containing sulphur oxides at temperatures up to 800 °C [15].

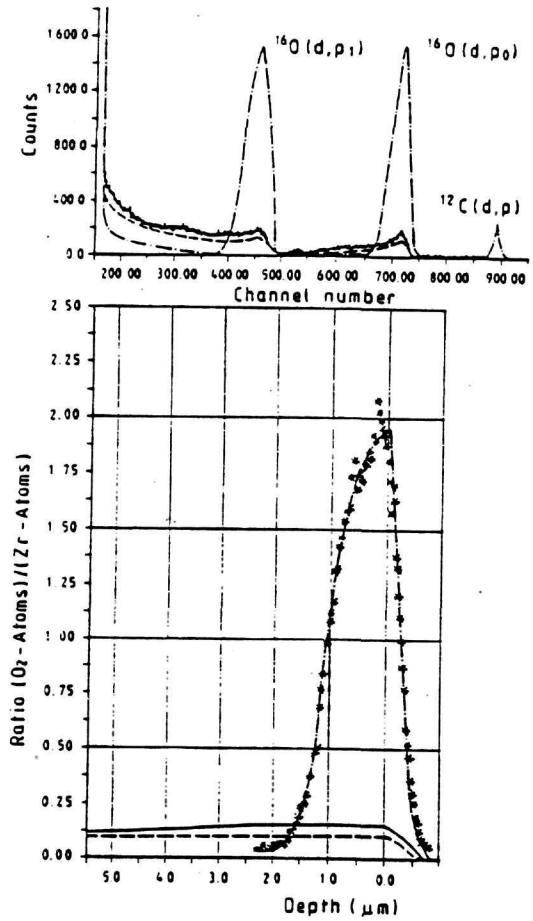

Fig. 4: Proton spectra and the oxygen distributions on treated Zr-surfaces (0, 1 and 2 days thermal treatment at 650 °C)

The Fig. 5 shows oxygen distributions on stainless-steel samples AISI 321 oxidized for different times at 750 °C in an aggressive atmosphere containing 80 % N_2, 17 % CO_2 and 3 % SO_2 (simulation of power industry process gases) [15].

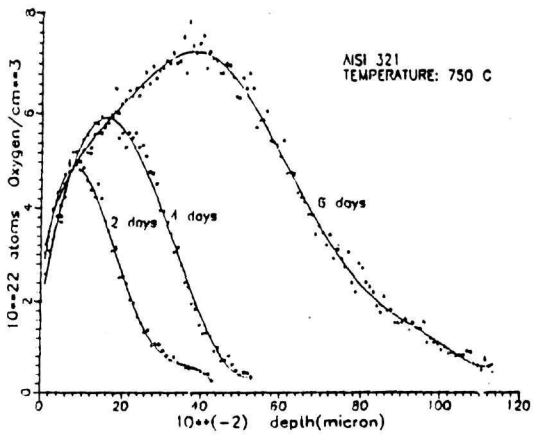

Fig. 5: Oxygen profiles on treated AISI 321 stainless-steel samples obtained by the reaction $^{16}O(d,p)^{17}O$

Of especial interest for the study of oxygen self-diffusion phenomena or very thin oxygen layers on materials surfaces is the $^{18}O(p,\alpha)^{15}N$ nuclear reaction. This reaction, studied initially studied for astrophysical purposes [16], found very wide applications to the materials science. This reaction on ^{18}O (natural abundance 0.2 %) shows at the projectile energies of 629, 833 and 1763 keV three narrow resonances [17]. Especially the resonance at 629 keV with a width Γ=2.1 keV has been proven to be a valuable tool in the investigation of oxygen providing depth resolutions near the surface between 500 and 2000 A in perpendicular geometry. The Fig. 6 shows the master excitation function of the reaction $^{18}O(p,\alpha)^{15}N$ for the 629 keV resonance at ϑ=150 ° recorded with a 50 A thick 75% ^{18}O-enriched Ta_2O target [18].

The elastic backscattering (RBS) is, most probably, the oldest ion beam technique. The Rutherford Backscattering Spectrometry and its applications are described in numerous specialized books and articles (e.g. 2, 5, 19) and is increasingly used for the solution of basic and industrial research problems [4].

An interesting effect for the determination of the distribution of the oxygen in thin surface layers of materials is the appearance of 5 resonances (s. Table 3) originating from the excitation of ^{20}Ne energy levels during the scattering of α-particles on ^{16}O [20]. This effect due not to Coulomb but to nuclear interactions can be used for analytical purposes [21, 22, 23].

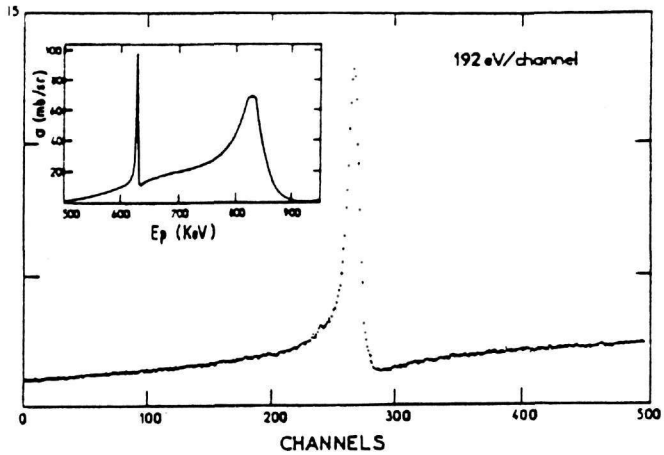

Fig.6 : Excitation function of the $^{16}O(p,\alpha)^{15}N$ nuclear reaction for the 629 keV resonance after (18).

Table 3: Resonances of the $^{16}O(\alpha,\alpha')^{16}O$ scattering reaction

Resonance Energy (MeV)	Γ_λ (keV)	^{20}Ne excitation energy (MeV)	J
E_r : 2.490	24	6.738	0^+
3.045	10	7.182	3^-
3.090	5	7.218	0^+
3.380	10	7.450	2^+
3.885	3	7.854	2^+

Especially the resonance at 3.045 MeV having high cross-section has been used for the profiling of oxygen in thin surface layers of metal and microelectronic materials. The elastic scattering spectrum of α-particles on a thin zirconium sample is given in Fig. 7.

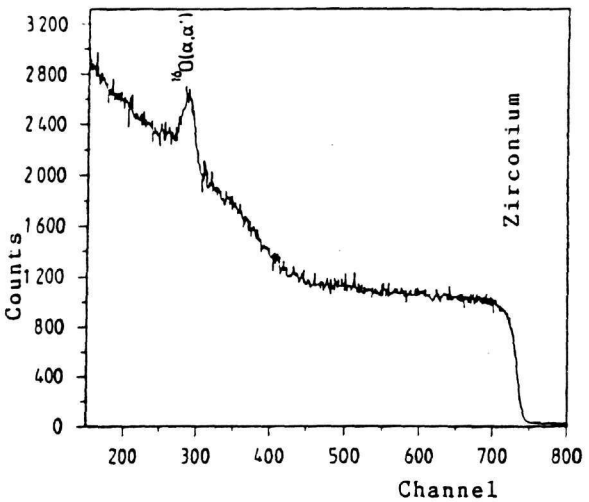

Fig. 7: Elastic scattering spectrum of α-particles on an thin oxide layer formed on zirconium (23)

The Elastic Recoil Detection Analysis (ERDA), that means the detection of the second particle involved in an elastic scattering process (the recoil) is also a valuable alternative to the RBS in the case of complicated matrix materials. With the proper selection of the projectile mass and energy, the recoil can escape from the substrate and be analysed for mass and energy (3, 4, 18). In order to achieve good transfer of energy to the recoiling nucleus the incident mass must be greater or comparable with the recoil mass.

Finally the Channeling technique can provide localization of the oxygen atoms in the microscopic level providing information about its atoms blocking structured channels in single crystals.

The evaluation of depth distribution data is not always an easy task because of the existance of overlapping peaks belonging to different reactions of the same or different nuclides. The carefull selection of the technique, the nuclear reaction and the experimental conditions are required for an increased reliability of the measurement. In the case of light projectiles straggling effects also dominate the interpretation of the excitation curves and must be taken into account. The depth resolution of the non-resonant nuclear reaction techniques is not very high. The resonant reactions offer in many cases much better depth resolution. Special simulation and deconvolution techniques have been developed to analyse the particle spectra obtained.

Conclusions

The accelerator-based analytical techniques, presented in this contribution taking as example the determination of the bulk concentration and depth distribution of oxygen, can:

1. Overbridge the analytical needs of the region covered by the atomic, electron and optical techniques from one side and the conventional bulk analysis.
2. Provide a re-evaluation of the nuclear physics data ensuring the high-precision required for the applications
3. Solve interesting interdisciplinary problems arising especially in the field of materials and solid state research
4. Find an attractive field of activity for small accelerators with limited possibilities for pioneering nuclear physics research work
5. Help the financial support of the laboratories and, with a good marketing attract applied research projects from industrial or governmental customers improving the relations research-production.

Acknowledgements

The technical assistance of the staff of the Tandem Accelerator Laboratory of NCSR DEMOKRITOS and the Nuclear Physics Institute of the University of Frankfurt / Germany is thankfully acknowledged. The performance of the experimental work hidden behind this simplified presentation of the methods would not be possible without the financial support of the General Secretariate of Research and Technology/Athens, the Stiftung Volkswagenwerk, the Federal Ministry of Research and Technology/Bonn (Internationales Buero- Forschungszentrum Juelich) and the Scientific Committee of NATO. Finally the above mentioned works would not be possible without the enthousiasm and the volunteering spirit of a number of graduate students and research scientists assisting during the experiments.

References

[1] G. Amsel et.al, Nucl.Instr. Methods **92** (1971) 481
[2] J.W.Mayer and E. Rimini (Eds), " Ion beam Handbook for Materials Analysis ", Academic Press, New York, 1977
[3] G. Deconninck, " Introduction to Radioanalytical Physics", Elsevier, Amsterdam-Oxford-New York, 1978
[4] T.W. Conlon, Contemp. Phys. **6** (1985) 521
[5] L.C.Feldman and J.W.Mayer, " Fundamentals of surface and thin film analysis", North-Holland, New York-Amsterdam-London, 1986
[6] P. Misaelides, J. Krauskopf, G. Wolf and K. Bethge, Nucl. Instr. Methods in Physics Research **B18** (1987) 281
[7] J. Krauskopf, P. Misaelides, G. Wolf, J. Meyer, V. Lieb-

ler. Proc. E-MRS Meeting, Strasbourg, 1987, Vol XVI, p. 469-473, Les Editions de Physique, Paris, 1987

[8] M. Valladon and J.L. Debrun, J. Radianal. Chem. **39** (1977) 385.

[9] J.P.C. Heggie et.al., Nucl.Instr. Meths **168** (1980) 125

[10] J. Lorenzen, Nucl.Instr. Meths **136** (1976) 289

[11] H.J. Rath et. al., J. Electrochem. Soc. **131** (1984) 1920

[12] G. Amsel, D. Samuel, Anal. Chem. **39** (1967) 1689

[13] A. Niiler and R. Birkmire, Nucl.Instr.Meths **149** (1978) 301

[14] P. Misaelides, A. Goncalves, H. Muenzel: "The oxidation of Zirconium", Intern. Conf. on Analytical Chemistry in Nuclear Technology, Karlsruhe, 1985 (will published in complete form,1991)

[15] Ch. Tsartsarakos, F. Noli, Doctoral Thesis (private communication).

[16] H. Lorenz-Wirzba et.al., Nucl.Phys. **A313** (1979) 346

[17] N.S. Christensen et. al., Nucl.Instr.Meths in Physics Research **B51** (1990) 97

[18] G. Amsel, W.A. Lanford: "Nuclear Reaction Analysis Techniques in Materials Analysis" in Ann. Rev. Nucl.Part.Phys. **34** (1984) 435

[19] W.K. Chu, J.W. Mayer, M.A. Nicolet: " Backscattering Spectrometry", Academic Press, New York, 1978

[20] J. R. Cameron: Phys. Rev **90** (1953) 839

[21] S. Petersonn et. al., Nucl.Instr.Meths **149** (1978) 285

[22] G. Possnert et.al., Physica Scripta **18** (1978) 353

[23] A. Novak, P. Misaelides, K. Bethge, Jahresbericht 1984, IKF-44 (1985) 45, Univ. Frankfurt, 1985.